Original Article

Asian Pacific Journal of Tropical Biomedicine

journal homepage: www.apjtb.org

doi: 10.4103/2221-1691.360564

Impact Factor: 1.51

Inhibition mechanisms of secretome proteins from *Paenibacillus polymyxa* Kp10 and *Lactococcus lactis* Gh1 against methicillin-resistant *Staphylococcus aureus* and vancomycin-resistant *Enterococcus*

Nurul Hana Zainal Baharin[1,2], Nur Fadhilah Khairil Mokhtar[1], Mohd Nasir Mohd Desa[1,2]✉, Nurul Diana Dzaraly[2], AbdulRahman Muthanna[2], Mazen M. Jamil Al-Obaidi[3], Mohd Hafis Yuswan[1], Sahar Abbasiliasi[1], Norasfaliza Rahmad[4], Wan Ahmad Kamil Wan Nur Ismah[5], Amalia Mohd Hashim[1,5], Shuhaimi Mustafa[1,5]

[1]*Laboratory of Halal Science Research, Halal Products Research Institute, Universiti Putra Malaysia, 43400 UPM Serdang, Selangor, Malaysia*

[2]*Department of Biomedical Sciences, Faculty of Medicine and Health Sciences, Universiti Putra Malaysia, 43400 UPM Serdang, Selangor, Malaysia*

[3]*Department of Science, University of Technology and Applied Sciences, Rustaq 10 P.C. 329, Oman*

[4]*Agro-Biotechnology Institute, Malaysia, National Institutes of Biotechnology Malaysia, 43400 UPM Serdang, Selangor, Malaysia*

[5]*Department of Microbiology, Faculty of Biotechnology and Biomolecular Science, Universiti Putra Malaysia, 43400 UPM Serdang, Selangor, Malaysia*

ABSTRACT

Objective: To determine the inhibition mechanisms of secretome protein extracted from *Paenibacillus polymyxa* Kp10 (Kp10) and *Lactococcus lactis* Gh1 (Gh1) against methicillin-resistant *Staphylococcus aureus* (MRSA) and vancomycin-resistant *Enterococcus* (VRE).

Methods: The sensitivity and viability of MRSA and VRE treated with secretome proteins of Kp10 and Gh1 were determined using minimal inhibitory concentration, minimum bactericidal concentration, and time-to-kill assays. The morphological changes were observed using scanning electron microscopy and transmission electron microscopy. To elucidate the antimicrobial mechanism of secretome protein of Kp10 and Gh1 against MRSA and VRE, 2D gel proteomic analysis using liquid chromatography-mass spectrometry was run by comparing upregulated and downregulated proteins, and the proton motive force study including the efflux of ATP, pH gradient, and the membrane potential study were conducted.

Results: MRSA and VRE were sensitive to Kp10 and Gh1 secretome protein extracts and displayed apparent morphological and internal composition changes. Several proteins associated with cellular component functions were either downregulated or upregulated in treated MRSA and VRE by changing the membrane potential gradient.

Conclusions: Kp10 and Gh1 secretome proteins reduce the growth of VRE and MRSA by damaging the cell membrane. Cell division, cell wall biosynthesis, and protein synthesis are involved in the inhibition mechanism.

KEYWORDS: Antimicrobial; Proteins; Secretome proteins; Antibiotic-resistance; *Paenibacillus polymyxa*; Kp10; *Lactococcus lactis*; Gh1; Vancomycin-resistant *Enterococcus*; Methicillin-resistant *Staphylococcus aureus*; Mechanism

Significance

This study provides valuable insight into the mechanisms by which growth and pathogenicity in methicillin-resistant *Staphylococcus aureus* and vancomycin-resistant *Enterococcus* are inhibited. This confirms the multifactorial effects of secretome protein extracted from *Paenibacillus polymyxa* Kp10 (Kp10) and *Lactococcus lactis* Gh1 (Gh1) on bacterial cells, suggesting their promising potential as a therapeutic agent for combating antibiotic-resistant pathogens.

✉To whom correspondence may be addressed. E-mail: mnasir@upm.edu.my

How to cite this article: Zainal Baharin NH, Khairil Mokhtar NF, Mohd Desa MN, Dzaraly ND, Muthanna AR, Al-Obaidi MMJ, et al. Inhibition mechanisms of secretome proteins from *Paenibacillus polymyxa* Kp10 and *Lactococcus lactis* Gh1 against methicillin-resistant *Staphylococcus aureus* and vancomycin-resistant *Enterococcus*. Asian Pac J Trop Biomed 2022; 12(11): 483-494.

Article history: Received 5 August 2022; Revision 24 August 2022; Accepted 16 October 2022; Available online 21 November 2022

1. Introduction

Antibiotic resistance among pathogenic bacteria has become a serious global public health threat. Vancomycin-resistant *Enterococcus* (VRE) and methicillin-resistant *Staphylococcus aureus* (*S. aureus*) (MRSA) are among the most common antibiotic-resistant bacterial pathogens. They have resulted in a considerable number of deaths and financial burdens on health services[1-3]. Moreover, it significantly threatens the progress in medical advances[1,3,4]. The effectiveness of traditional antibiotics has declined drastically over time, and more effective therapeutic agents against infections due to antibiotic-resistant bacteria are desperately needed[4-6]. Attempts to identify substances that could replace the existing antibiotics are being made.

Secretome proteins are secreted out of cells and are reported to have antimicrobial activity as they contain antimicrobial compounds that can inhibit bacterial growth and could potentially replace antibiotics[7]. As antibiotic-resistance cases are increasing, the use of secretomes can be one of the alternatives to prevent drug resistance. Some studies have shown that secretomes contain antimicrobial peptides (AMPs) such as cathelicidin, RNase3, human β-defensins, and calprotectin[8]. For example, the secretome of adipose tissue could suppress the growth of *S. aureus* by increasing activity of cathelicidin[9,10].

AMPs in secretome proteins act as host defenses, where most of them have been isolated from eukaryotes, such as animals, plants, and fungi[3,11]. Some bacteria contain secretome proteins and could inhibit food-borne pathogens and other pathogenic bacteria[12]. For example, the use of secretomes from bacteria found in skin wounds could inhibit the growth of gram-positive *S. aureus* and gram-negative *Escherichia coli*[10].

Meanwhile, studies have demonstrated the ability of certain bacterial groups to inhibit the growth of some pathogenic microorganisms and degrade mycotoxins. Also, studies have described probiotic properties and the antimicrobial activity of the cell-free extracts of the bacterial strains isolated from various sources[12]. Although some bacterial strains have been widely used as culture starters and bacteriocins as food preservatives, more studies on the inhibitory potential of probiotic bacteria against antibiotic-resistant pathogens are needed. It is thus important to leverage new technologies to characterize and identify new bacterial strains that demonstrate stronger antimicrobial effects against antibiotic-resistant bacteria.

Paenibacillus polymyxa Kp10 (Kp10) and *Lactococcus lactis* Gh1 (Gh1) both are probiotic bacterial isolates that have previously exhibited antimicrobial activity and could potentially replace antibiotics[13,14]. Gh1 was reported to inhibit the pathogenic *S. aureus*, *Listeria monocytogenes*, *Salmonella*, and *Bacillus cereus*[15]; while Kp10 was screened to have antimicrobial activity against *Escherichia coli*[13]. Therefore, the secretome proteins of these strains are of interest to be investigated for their mechanistic actions. This study seeks to explore the antimicrobial characteristics of the secretome protein extracts of Kp10 and Gh1, and their potential to inhibit antibiotic-resistant pathogens VRE, and MRSA. The results of this study may help to ultimately develop antimicrobial alternatives and reduce dependence on conventional antibiotics.

2. Materials and methods

2.1. Bacterial culture, growth, and storage conditions

MRSA (ATCC 700699) and VRE (ATCC 700221) were obtained from the American Type Culture Collection (ATCC). Inoculates of MRSA and VRE were prepared using the colony suspension method. Colonies were picked from cultures that had previously grown on Mannitol Salt Agar and sheep blood agar for 24 h at 37 ℃[16] and transferred to brain heart infusion (BHI) broth before incubating for 24 h at 37 ℃. Kp10 and Gh1 isolates were kindly provided by Arbakariya Ariff, from the Bioprocessing and Biomanufacturing Research Centre, Faculty of Biotechnology and Biomolecular Sciences, Universiti Putra Malaysia. Kp10 was cultured in M17 broth at 37 ℃ while Gh1 was cultured in MRS broth at 37 ℃[13,17].

2.2. Preparation of secretome proteins from cell-free culture supernatant of Kp10 and Gh1

Secretome proteins from Kp10 and Gh1 were extracted and purified from the cell-free culture supernatant of the bacteria using the ammonia sulphate precipitation method[18]. Firstly, Kp10 and Gh1 were cultured in M17 broth and MRS broth, respectively for 24 h at 37 ℃. Then, 1 000 mL of cultured bacteria suspension were aliquoted into 50 mL falcon tubes and centrifuged at 10 000×*g* at 4 ℃ for 15 min. All cell-free supernatants were collected into a sterile bottle, where 567 g $(NH_4)_2SO_4$ was added and stirred using a magnetic stirrer (Thermo Fisher Scientific, United States) until they were fully dissolved. The solution was subsequently aliquoted into 50 mL tubes and incubated overnight at 4 ℃. Following incubation, the tubes were centrifuged at 10 000×*g* at 4 ℃ for 15 min. Supernatants were removed from the precipitate and replaced with distilled water. The tubes were stored overnight at 4 ℃. Finally, the content of all tubes was mixed into one large beaker for inoculum preparation. The concentration of the secretome proteins was determined by using the Bradford assay.

2.3. Determination of minimum inhibitory concentration (MIC) and minimum bactericidal concentration (MBC)

MIC and MBC were determined using the Resazurin-based 96-well plate microdilution method[19]. Resazurin was prepared in

distilled water at 0.02% (*w/v*), sterilized by filtration, and stored at 4℃ for up to two weeks after preparation. The direct colony suspension method was used to prepare a saline suspension of the organism at the density of the McFarland 0.5 turbidity standard, which corresponded to 1×10^8-2×10^8 CFU/mL. Plates were prepared aseptically, and a sterile 96-well plate was labeled. A volume of 100 µL of the test material was pipetted into the first row of the plate (well 1). In the case of the other wells, 50 µL of Mueller Hinton broth was added (wells 2-12). Serial dilution was performed using a multichannel pipette, starting from well 1 and ending at well 10. Wells 11 and 12 were used as negative controls. The concentrations of the different samples were achieved through doubling serial dilution. Finally, 1 µL of tested bacteria was added to each well. Following overnight incubation at 37℃, 30 µL of resazurin (0.02%) was added to all wells. This was followed by a further incubation period lasting 2-4 h to observe any color change. MIC was defined as the lowest concentration of the test material that could prevent any color change. Columns with no color change (the blue resazurin color remained unchanged) after incubation were scored as MIC values. The presence of pink and purple colors indicated growth, whereas the presence of blue colors indicated growth inhibition. By directly plating the contents of the well with a concentration that exceeded the MIC value, MBC was determined. The MBC value was determined after no colony growth occurred from the directly plated contents of the wells.

2.4. Time–to–kill assays

Time-to-kill assays were performed as of CLSI guidelines and previously described methods[20]. Bacterial cell cultures were suspended in BHI broth overnight and adjusted to an absorbance of about 10^6 CFU/mL. Secretome proteins of Kp10 and Gh1 were added to inoculum suspensions at final concentrations corresponding to 1×MIC and incubated at 37℃. After 0, 2, 4, 8, 12, and 24 h of incubation, aliquots were taken from the inoculum cultures. They were serially diluted, plated on MH agar, and incubated at 37℃ for 24 h. The colony count was used to determine the viability of bacterial cells. The tests were carried out in triplicate. The viability of the cells was calculated as a percentage.

2.5. Preparation of MRSA and VRE treated with Kp10 and Gh1

MRSA and VRE were cultured in BHI broth and incubated for 24 h at 37℃. The culture was then subdivided into 50 mL aliquots before treatment with secretome proteins from Kp10 and Gh1 for 12 h (50% viability according to time to kill assays) or left untreated as a control.

2.6. Scanning electron microscopy (SEM) and transmission electron microscopy (TEM) analysis

Treated cells were then centrifuged and supernatants were decanted to obtain pellets. The samples were allowed to fix in 2.5% glutaraldehyde for 4-6 h at 4℃. For SEM, following fixation, samples were washed with 0.1 mol/L sodium cacodylate buffer 3 times (10 min each) with supernatant decanted in each step. The samples were then post-fixed with 1% osmium tetroxide for 2 h at 4℃ for post-fixation. Then, samples were washed again with 0.1 mol/L sodium cacodylate buffer 3 times. Subsequently, the samples were dehydrated in ascending grades of acetone dilution (35%, 50%, 75%, 95%, and 100%). After dehydration, the samples were pipetted onto aluminum foil of 1 cm diameter coated with albumin and were left to dry in a critical point dryer for 1 h and 30 min. Finally, they were mounted onto the stub using double-sided tape and sputter-coated with gold coating before they were examined under the SEM using JSM-IT100 InTouchScope™ SEM (JOEL Ltd, Japan).

As for TEM, following fixation, animal serum was added to the samples, and they were allowed to clot. The clotted samples were subsequently diced into 1 mm^3 size and fixed in 2.5% Glutaraldehyde for 1-2 h at 4℃. The next few steps (washing, post-fixation, washing & dehydration) were carried out similar to the SEM protocols. Following dehydration, samples were infiltrated with an increasing concentration of acetone and resin mixture and embedded into a beam capsule filled with resin. A glass knife and ultramicrotome were utilized to cut 1 µm thick sections of the sample. The thick sections were then placed onto a glass slide, stained with toluidine blue, and examined under a light microscope (Olympus, Japan). The areas of interest were selected and cut for ultrathin sections. The silver sections were subsequently selected and picked up using a grid. Finally, the sections were stained with uranyl acetate for 15 min (washed twice with distilled water) and lead stain for 10 min (washed twice with distilled water) before they were viewed under TEM.

2.7. Proton motive study

2.7.1. Membrane potential assay

The membrane potential ($\Delta\psi$) of MRSA and VRE cells was quantified qualitatively using the potentiometric fluorescent probe 3,39-dipropylthiadicarbocyanine iodide [(DiSC3(5)] (Molecular Probes Inc, Eugene, OR). Firstly, cells were harvested in the log phase (optical density at 660 nm). Then the cells pellets were washed twice with ice-cold 50 mmol/L potassium 4-(2-hydroxyethyl) piperazine-1-ethanesulfonic acid (K-HEPES) buffer, pH 7.0, and resuspended in the same buffer to 1/100 of their initial volume with 1% sucrose solution and kept on ice. Then, the glucose-energized bacterial cells were added to a 96 wells plate containing 100 µL K-HEPES buffer and 10 µL DiSC3(5) (5

mmol/L) in each well. Plates were monitored with fluorescence measurements using a Synergy H1 multi-mode microplate reader (BioTek, United States) with a 5 nm band-pass width and excitation and emission wavelengths of 643 and 666 nm, respectively. After baseline fluorescence was recorded, 2 μL nigericin (1.5 nmol/L) was added to dissipate the pH gradient, followed by addition of Kp10 and Gh1 secretome proteins to the desired final concentration, and measurements were recorded for an additional 30 min. Wells containing a medium with 10 μL DiSC3(5) and dimethyl sulfoxide, followed by the addition of secretome proteins extract (1×MIC) were made as the control.

2.7.2. Monitoring intracellular pH with BCECF

To determine the pH gradient of the transmembrane, MRSA and VRE cells (OD_{660}, 0.6) were loaded with the fluorescent probe 20-70-bis(carboxyethyl)-5(6)-carboxyfluorescein acetoxymethylester (BCECF AM) (Molecular Probes Inc., Eugene OR) and subjected to an acid shock. Glucose-energized (1% sucrose solution), BCECF-loaded cells (OD_{660}, 0.6) were added to a 96 wells plate containing 100 μL of 50 mmol/L Kpi buffer (pH 6.0). The Δψ was then dissipated with vancomycin (8 μg/mL) and secretome proteins extract (1×MIC). Fluorescence was measured with band-pass widths of 5 and 15 nm and wavelengths of 500 and 525 nm for excitation and emission, respectively.

2.7.3. Measurement of adenosine triphosphate (ATP) efflux

The detection of ATP efflux was based on a bioluminescence assay in which MRSA and VRE cells were grown in 25 mL of BHI broth at 37℃ until absorbance ranged from 0.6 to 1.0 at 600 nm. Bacterial cells were centrifuged at 3 000 *g* for 10 min before being washed twice with 50 mmol/L 2-(*N*-morpholino) ethanesulfonic acid buffer, pH 6.5, and suspended in 2.5 mL of a 10 mmol/L KCl solution containing 1% (*w/v*) *D*-glucose. To measure total ATP, 20 μL of MRSA and VRE cell suspension was mixed with 80 μL of dimethyl sulfoxide and diluted with 4.9 mL of distilled water[21]. For extracellular ATP measurement, 20 μL of bacterial cell suspension was mixed with 50 mmol/L HEPES buffer, pH 6.5, and 100 μL of this suspension was mixed with 100 μL of the ATP solution (Life Technologies, United States). Then, this suspension was added with different concentrations of both secretome proteins and nisin as the positive control (0.25, 0.5, 1×MIC). As a negative control, the HEPES buffer and ATP solution (without the secretome protein or nisin) were only used to be added in the experimental cells. All samples were uploaded to 96 well plates and 100 μL of luciferase enzyme was then added to each of the samples. The light produced was measured by using a Synergy H1 multi-mode microplate reader (BioTEK, United States) after 30 min. The excitation and emission spectra were recorded between 250-500 nm (λ_{em}=530 nm) and 450-650 nm (λ_{ex}=390 nm), respectively. The standard curve was created using the ATP assay kit's standard ATP (Life Technologies, United States).

2.8. Protein identification from two-dimensional (2-DE) electrophoresis and gel image analyses by using liquid chromatograph/mass spectrometer (LC-MS)

The proteomic analysis of MRSA and VRE treated by secretome proteins of Kp10 and Gh1 was intended to elucidate some unusual mechanism or dynamic behavior of this bacteria. Samples were taken for 2-DE analysis to identify and quantify protein expressions in each treated cell. Different protein spots resulting from the secretome proteins-treated MRSA and VRE were excised from 2-DE gels and analyzed by peptide mass fingerprinting using LC-MS. The proteins were deduced based on protein-protein interactions predicted using Search Tool in the Retrieval of Interacting Genes/Proteins (STRING) database v9.0 (http://www.string-db.org/).

2.8.1. Extraction of MRSA and VRE treated with secretome proteins

Lysis buffers were made by combining 10.5 g of 7 mol/L urea, 3.8 g of 2 mol/L thiourea, 1.0 g of 4% 3-(3-cholamidopropyl)-dimethylammoniopropane sulfonate, 500 μL of 2% IPG buffer, and 154 mg of 40 mmol/L dithiothreitol (DTT) in 25 mL of distilled water. After that, treated cells were harvested by centrifugation, and supernatants were decanted. To prevent heating, 1 mL of lysis buffer was added to the pellet and sonicated 10 times for 15 s at 20% power while the sample was kept in iced water. After that, the protein suspension was centrifuged at 15 000×*g* for 4 min at 4℃. The pellet was discarded, and the supernatant was collected as the secretome protein extract. The protein concentration of the secretome protein extract was determined using Bradford assays, and the absorbance was measured at 595 nm using a 96-well microplate reader (Tecan, Männedorf, Switzerland) with different dilutions of bovine serum albumin as the standard. By comparing the sample absorbance to the standard curve, the concentration of the unknown samples was calculated.

2.8.2. 2-DE electrophoresis and gel image analyses

The 1st-dimensional separation was performed using 13 cm IPG strips (Immobiline® pH 4–7, GE Healthcare, United States) and the Ettan Ipghor Ⅱ isoelectric focusing system (Amer-sham Bioscience, United Kingdom). A total of 300 g of protein was loaded onto the strips, and isoelectric focusing was performed at 20℃ at 1 h for 500 V, 1 h for 1 000 V, and 1 h for 8 000 V. The strips were equilibrated twice with 10 mg/mL DTT and 25 mg/mL iodoacetamide before the 2nd-dimension separation. The second-dimensional separation was performed at 10 mA/gel for 15 min and then at 20 mA/gel for 3 h on a Ruby SE 600 vertical electrophoresis system (GE Healthcare, United States) with a full-

range rainbow molecular weight marker (GE Healthcare, United States) as the standard. The gels were stained with Coomassie staining after being fixed in 50% (*v/v*) ethanol in 10% acetic acid overnight, stained with 0.02% Coomassie Blue R-250 for 6 h, and then destaining with 7% acetic acid in 40% ethanol for 30 min. The gels were imaged using a GS-800 Calibrated Densitometer (Bio-Rad Laboratories, United States) with a 32-bit pixel depth and 300 dpi resolution. Progenesis Same Spot software (Nonlinear Dynamics, Netherlands) and one-way analysis of variance were used to analyze the protein profiles of four biological replicates at different time points from each pair (ANOVA). Spots with significant changes (P<0.05 and fold-change value > 2) were chosen for identification[22,23].

2.8.3. Spot picking and in-gel digestion

Selected protein spots were excised from 2-DE gels and stored in the chiller in a gel plug storage solution. Gel plugs were washed for 10 min with 100 mmol/L ammonium bicarbonate (ABC). Gel plugs were then de-stained twice for 15 min each time with a freshly prepared solution containing 15 mmol/L $K_3Fe(CN)_6$ and $Na_2S_2O_3$ in water. The gel plugs were then incubated for 30 min at 60 ℃ in a reduction solution containing 10 mmol/L DTT in 100 mmol/L NH_4HCO_3 before being alkylated for 20 min at 26 ℃ in the dark with 55 mmol/L iodoacetamide in 100 mmol/L NH_4HCO_3. The gel plugs were then dehydrated with 50% *v/v* acetonitrile (ACN) in 100 mmol/L ABC twice for 20 min each, followed by a 15-min incubation with 100% *v/v* ACN at room temperature. The gel plugs were vacuum-dried and hydrated for 10 min at room temperature (26 ℃) in 10 mL trypsin solution (12.5 ng/mL trypsin in 25 mmol/L ABC). At 37 ℃ in a water bath, the sample was incubated overnight for digestion. The sample was then dehydrated with 50% ACN for 15 min, followed by 100% ACN for 15 min, and the supernatant containing the digested protein was transferred to new tubes and vacuum-dried later[22,23].

2.8.4. Protein identification using LC-MS/MS

The freeze-dried sample was dissolved in 40 μL of 0.1% trifluoroacetic acid (TFA) and sonicated for 30 s on/30 s off with a high setting for 10 min each while on ice water. The sample was then centrifuged at 19000×*g* for 15 min at 4 ℃, and the supernatant of the dissolved sample was desalted by using a zip tip. The peptide was eluted using 50% ACN and 0.1% TFA, and this supernatant was further freeze-dried. A volume of 20 μL of 3% ACN and 0.1% formic acid (FA) was added to the dried sample. The samples were then analyzed with a quadrupole Orbitrap benchtop mass spectrometer (Q-Exactive, Thermo Scientific, United States) equipped with an EASY-nLC 1000 system (Thermo Scientific, United State). The tryptic peptides from the dimethylated samples were injected directly into an analytical column (C18, particle diameter 3 μm, 0.075 mm×125 mm; Nikkyo Technos, Japan). Using an EASY-nLC 1000, tryptic peptides were separated with a gradient of buffers A (0.1% FA) and B (0.1% FA and 90% ACN) (0-29 min, 5%-30% B; 29-37 min, 30%-55% B; 37-38 min, 55%-80% B, and 38-40 min, 80% B) at a flow rate of 300 nL/min. Peptides were introduced to the Q-Exactive from the chromatography column. The spray voltage was 2 kV with no sheath or auxiliary gas flow, and an ion-transfer tube temperature of 250 ℃. MS1 spectra were collected at 140000 resolutions in the scan range of 350-1400 *m/z* to achieve an automatic gain control target of 3e6. The automatic gain control target value for fragment spectra was set to 2e5, while the intensity threshold remained at 2e3. The isolation width was set to 2.4 *m/z*, and the ten most intense ions were fragmented in a data-dependent mode using collision-induced dissociation with a normal collision energy of 27%. Tandem mass spectra were collected using the Orbitrap mass analyser (Thermo Scientific, United States), which has a mass resolution of 17500 at 200 *m/z*. The maximum allowed ion accumulation times for full MS scans were 100 ms and 50 ms for tandem mass spectra.

2.8.5. Metabolic prediction

Protein-protein interactions were predicted using STRING database v9.0 (http://www.string-db.org/). The Swiss-Prot identifier for the *S. aureus* and enterococci genes in "protein mode" was used to search against the STRING database. Network analysis was set at medium stringency (STRING score=0.4). Proteins were linked based on seven criteria: neighborhood, gene fusion, co-occurrence, co-expression, experimental evidence, existing databases, and text mining. The functional study of identified proteins and their classification into functional categories were performed using the databases Universal Protein Resource (UniProt) (UniProt Consortium, 2015) and COGNITOR to identify the Clusters of Orthologous Groups of proteins.

2.9. Statistical analysis

All experiments were performed in triplicate. In 2-DE gel analysis, one-way analysis of variance was used to analyze the protein profiles of four biological replicates at different time points from each pair (ANOVA). Spots with significant changes were identified based on P<0.05 and fold-change value. In time-to-kill assay and proton motive study, all data were expressed as mean±standard deviation. Data were analyzed by ANOVA followed by Tukey's *post hoc* tests using IBM SPSS Statistics® version 21 (Armonk, NY, United States) and Microsof Excel version 2019. P<0.05 was considered significant.

3. Results

3.1. In vitro antimicrobial activity of secretomes from Kp10 and Gh1 against MRSA and VRE

MICs of Kp10 secretome against MRSA and VRE ATCC strains

were 0.15 and 0.36 μg/mL, respectively; while MICs of Gh1 secretome against MRSA and VRE were 2.95 and 1.48 μg/mL, respectively.

MBCs of Kp10 secretome against MRSA and VRE ATCC strains were 0.16 and 0.69 μg/mL, respectively; while MBCs of Gh1 secretome against MRSA and VRE were 5.10 and 2.95 μg/mL, respectively.

3.2. Time-to-kill assay

In this study, the time-to-kill assay showed that the Kp10 and Gh1 secretome proteins exhibited significant bactericidal activity at 1×MIC in a time-dependent manner (Figure 1). After 8 h of incubation, MRSA growth was reduced to less than half of 50% as exhibited in the time-kill curve in the graph. There was a declining trend in growth observed at every 2 h interval within 12 h of

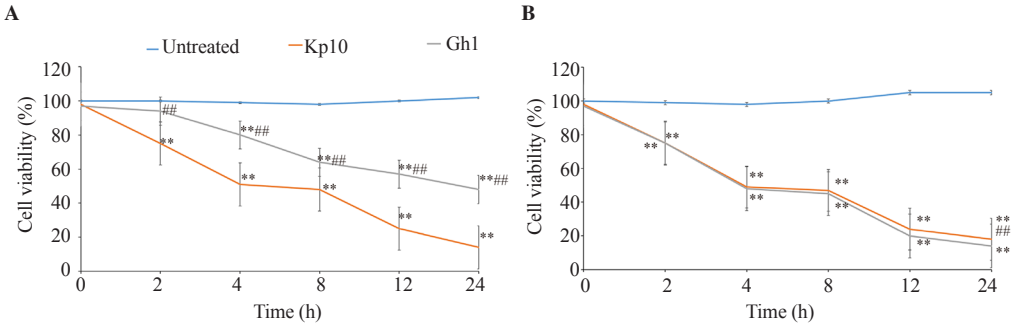

Figure 1. Percentage of viability measured by time-to-kill assay. A: MRSA; B: VRE. Values were presented as mean±standard deviation of triplicate experiments. Significant differences were analyzed by one-way ANOVA test followed by Tukey's multiple comparison. $^{**}P<0.01$, compared with untreated cells; $^{\#\#}P<0.01$, compared with cells treated with secretome protein of Kp10. MRSA: methicillin-resistant *Staphylococcus aureus*; VRE: Vancomycin-resistant *Enterococcus*.

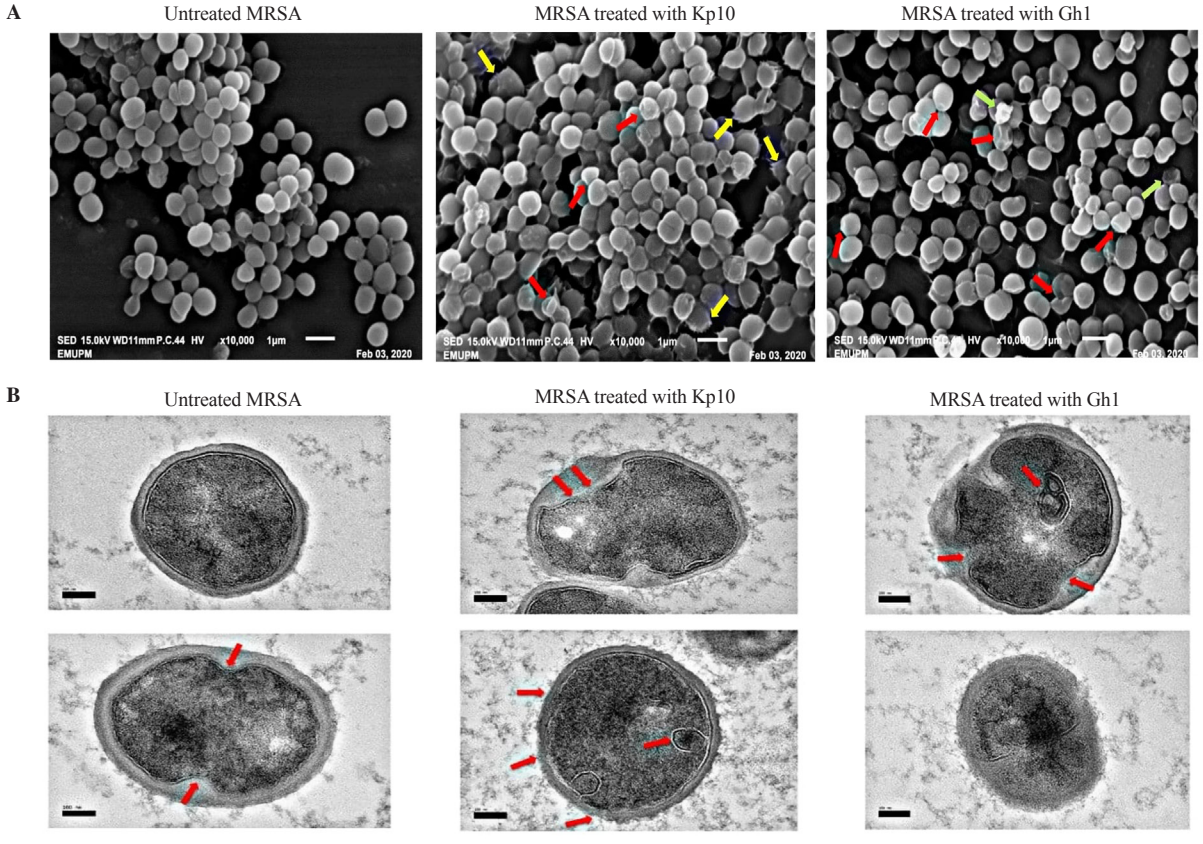

Figure 2. (A) SEM images of untreated MRSA and MRSA treated with secretome proteins of Kp10 and Gh1. Scale bar corresponds to 1 μm. (B) TEM images of untreated MRSA and MRSA treated with secretom proteins of Kp10 and Gh1. Scale bar corresponds to 100 nm. Magnification: 20000×. There was spheroplast (yellow arrow), pitted membrane (red arrow), and lysis of some cells (green arrow) in Figure 2A; while there was swelling in the periplasmic space and some mesosomelike structures (red arrow) in Figure 2B.

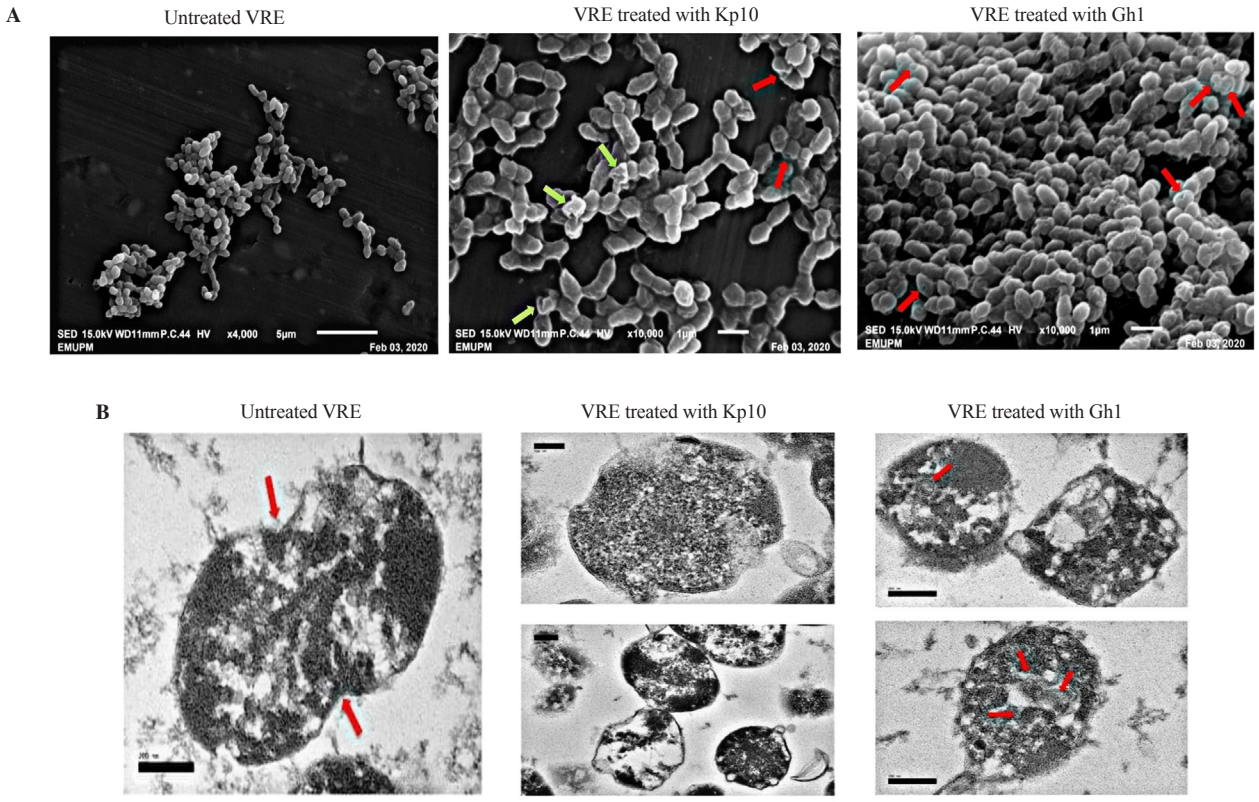

Figure 3. (A) SEM images of untreated VRE and VRE treated with secretome proteins of Kp10 and Gh1. Scale bar corresponds to 1 µm. (B) TEM images of untreated VRE and VRE treated with secretom proteins of Kp10 and Gh1. Scale bar corresponds to 100 nm. Magnification: 20000×. Some completely burst cells were observed (green arrow). The surface of bacterial cell appeared to be aggregated with dimples and blisters. The treatment also caused abundant pitting of membranes (red arrow).

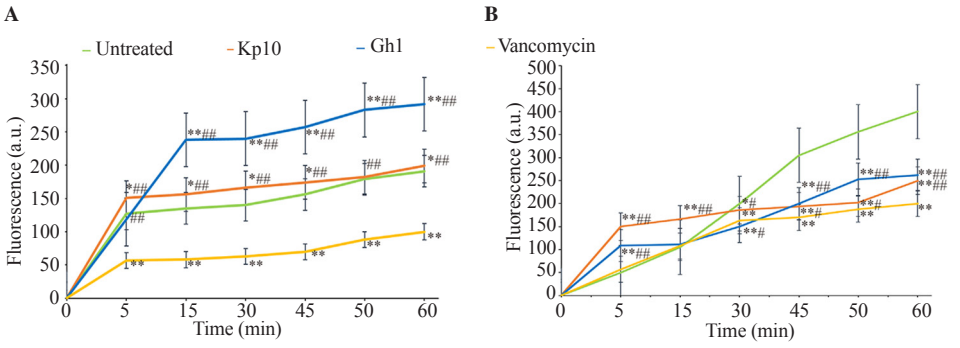

Figure 4. Membrane potential of MRSA (A) and VRE (B). The data were presented as mean±standard deviation of triplicate experiments. Significant differences were analyzed by one-way ANOVA test followed by Tukey's multiple comparison. $^{*}P<0.05$ and $^{**}P<0.01$, compared with untreated cells; $^{\#}P<0.05$ and $^{\#\#}P<0.01$, compared with cells treated with vancomycin.

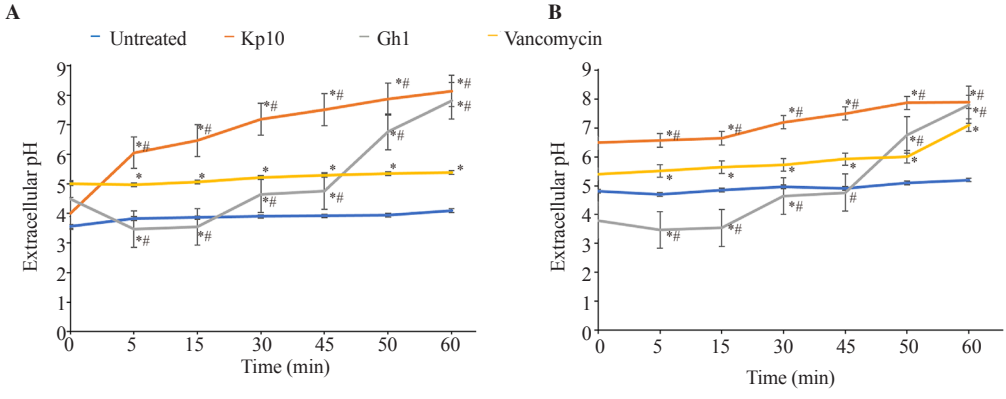

Figure 5. Effect of secretome protein on the pH gradient of MRSA (A) and VRE (B). The data were presented as mean±standard deviation of triplicate experiments. Significant differences were analyzed by one-way ANOVA test followed by Tukey's multiple comparison. $^{*}P<0.05$, compared with untreated cells; $^{\#}P<0.05$, compared with cells treated with vancomycin.

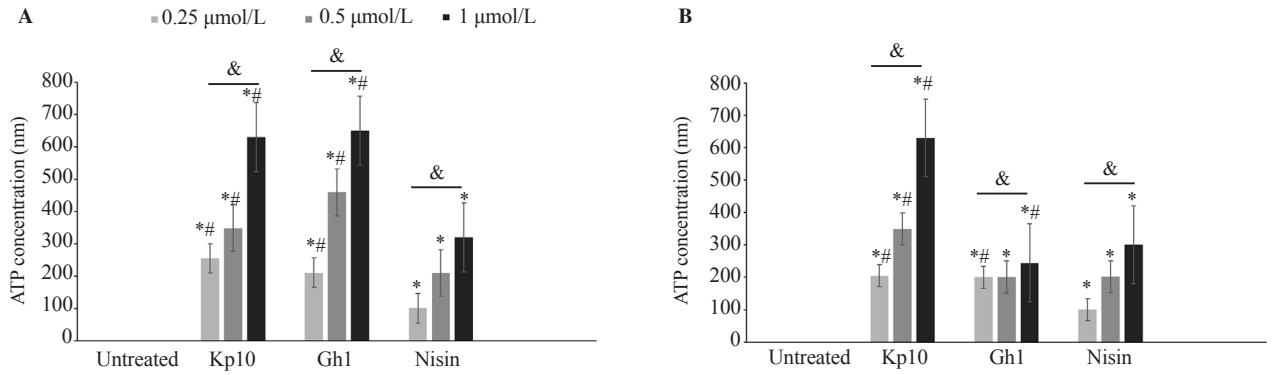

Figure 6. Efflux of ATP of MRSA (A) and VRE (B). The data were presented as mean±standard deviation of triplicate experiments. Significant differences were analyzed by two-way ANOVA test followed by Tukey's multiple comparison. $^{*}P<0.05$, compared with untreated cells; $^{\#}P<0.05$, compared with cells treated with nisin at the same concentration; $^{\&}P<0.05$, significant difference between each concentration in treated group.

Table 1. Protein identificantion by LC-MS.

ID	*P* value	Accession No	Protein identity	Identified pl/Mw (KDa)	Theoretical pl/Mw (KDa)	Unique peptides
MRSA						
1426	0.009	YP_500964.1	50S ribosomal protein L6	9.97/15	9.54/19	1
1728	0.047	YP_500324.1	Putative universal stress protein SAOUH-SC_01819	7.34	5.60/18	2
786	0.004	YP_499171.1	Alcohol dehydrogenase	6.99/27	5.34/36	1
		YP_499972.1	*L*-threonine dehydratase catabolic TdcB		6.08/37	1
859	0.020	YP_499671.1	Ornithine carbamoyltransferase	5.38/25	5.06/37	1
1354	0.043	YP_501405.1	ABC transporter, ATP-binding protein, putative	4.79/17	7.92/27	1
669	0.044	YP_501046.1	Uncharacterized protein	6.45/31	5.91/30	1
		YP_499352.1	Phosphoglycerate kinase		5.17/42	1
834	0.036	YP_500103.1	Segregation and condensation protein B	4.77/25	4.30/20	1
VRE						
1358	0.047	WP_002289688.1	Pyruvate dehydrogenase complex	4.48/33	4.62/35	1
1358	0.047	WP_002356760.1	Elongation factor Ts		4.87/32	6
1358	0.047	WP_002355904.1	Cell division protein DivIVA		4.53/26	1
2584	0.004	WP_002357967.1	50S ribosomal protein L31 type B	6.08/10	5.57/10	3
2584	0.004	WP_002355121.1	Cold-shock domain family protein		4.35/7	1
2058	0.044	WP_002356426.1	50S ribosomal protein L10	5.6/18	5.39/17	8
2058	0.044	WP_002356762.1	Ribosome-recycling factor		5.21/20	6
1912	0.028	WP_002356090.1	Gls24 protein	5.13/20	4.71/20	9
1912	0.028	WP_002387688.1	Superoxide dismutase [Fe]		4.99/22	4
1912	0.028	WP_002357972.1	Fructose-bisphosphate aldolase class-Ⅱ		4.86/30	3
827	0.025	WP_002362559.1	60 kDa chaperonin	4.64/54	4.64/57	16
827	0.025	WP_002357825.1	Chaperone protein DnaK		4.59/65	15
827	0.025	WP_002383741.1	Glutamine-fructose-6-phosphate aminotransferase		4.92/65	2
2479	0.032	WP_002356203.1	50S ribosomal protein L23	3.89/12	9.62/11	5

incubation. Following 12 h of incubation, the growth started to diminish steadily until the growth ceased after 24 h of incubation. Similar results were obtained for VRE.

3.3. Microscopic analysis by using SEM and TEM

SEM image showed several damages to the surface of MRSA treated with Kp10 and Gh1 secretome proteins following 12 h of incubation. They appeared to be aggregated with dimples and blisters. There was also spheroplast (yellow arrow). The pitted membrane (red arrow) and lysis of some cells (green arrows) could also be observed (Figure 2A).

TEM analysis showed that the untreated bacterial cells displayed a well-defined spherical shape morphology and smooth surfaces with obvious boundaries between them where the inner and outer membranes were visible as continuous structures. The periplasmic space had a uniform appearance and was thin. Following 12 h treatment with Kp10 secretome proteins, the coccoid shape of MRSA was not preserved. The outer membrane was weakened but the inner membrane remained intact although slightly waved. There was also swelling in the periplasmic space and some mesosome-like structures (red arrow) could be observed. After treatment with

Gh1 secretome proteins, TEM showed the weakening of both the outer and inner cell membranes. Subsequently, the presence of double-layered mesosome-like structures could be observed in the cytoplasm. In addition, the periplasmic space was also swollen (Figure 2B).

SEM images exhibited smooth and intact surfaces with structural integrity in the untreated VRE. The diplococci shape of VRE was not preserved after 12 h of incubation of secretome protein. The bacterial cells also displayed surface irregularity and indentations (red arrow). Some completely burst cells were also observed (green arrow). The surface of bacterial cell appeared to be aggregated with dimples and blisters. The treatment also caused abundant pitting of membranes (red arrow) (Figure 3A).

In untreated VRE cells, cell wall and membrane were intact and there was no noticeable damage. TEM images confirmed remarkable changes in the shape and size of the cells after treatment. The membranes displayed partial disruption and permeabilization which leads to leakage of cell contents. The secretome proteins-treated bacterial cells also showed lytic effects. The enterococcal shape of VRE was severely compromised and there was clear deformation of the cell surface. Gh1 treatment for 12 h also caused the perforation of bacteria membrane at polar ends which subsequently leads to cytoplasm leakage. Double-layered mesosome-like structures were also seen in the cytoplasm (Figure 3B).

3.4. Proton motive study

Tests with the fluorescence probes DiSC3(5) and BCECF indicated that both secretome proteins had a significant impact on membrane potential ($\Delta\psi$) and ΔpH in MRSA and VRE. Vancomycin showed less effect on the fluorescence intensity of DiSC3(5) as compared with secretome proteins-treated MRSA and VRE (Figure 4). Tests with BCECF indicated that the Kp10 and Gh1 secretome proteins caused more dissipation of ΔpH (Figure 5). The efflux of ATP test indicated that the ATP concentration in the Kp10 and Gh1 secretomes-treated MRSA and VRE was higher than in untreated cells (Figure 6).

3.5. Protein identification from 2–DE electrophoresis and gel image analyses by using LC–MS

A total of 24 and 14 different protein spots from MRSA and VRE, respectively were excised from 2-DE gels and analyzed by peptide mass fingerprinting using LCMS. Table 1 summarizes identified proteins.

4. Discussion

MRSA and VRE have become common pathogens that are considered a hazard in inpatient care, particularly in the acute or long-term care setting[24]. However, treatment of MRSA and VRE infections with the current antibiotics has limitations due to the emergence of multidrug-resistant strains[25]. In this study, the secretome proteins extracted from Kp10 and Gh1 showed anti-MRSA and anti-VRE activities, with the view that the secretome proteins may contain AMPs as a promising therapeutic candidate against antibiotic-resistant bacteria[3,26].

The inhibitory activity of the secretome proteins, as revealed by *in vitro* MIC and MBC tests, was supported by the electron microscopy findings. The use of SEM and TEM may identify structural changes due to secretome proteins, revealing the antibacterial capability of diverse drugs. Based on the microscopic study, the changes in the bacteria cell membrane suggested the possibility of cytoplasm leakage, membrane damage, and loss of functionality associated with the effect of secretome proteins. A previous study showed that the perforations in the cell membrane caused potassium ions to exit the cell, which inhibited respiration and promoted propidium iodide uptake[27]. It was also suggested that AMPs from secretome proteins interact with the outer membrane by displacing Mg^{2+} ions from outer membrane component, lipopolysaccharide (LPS)[28]. The destabilization of the outer membrane eventually enables AMPs from the secretome proteins to fill the periplasmic space through the promotion of AMPs penetration. Whereas the creation of holes was attributed to an alteration in the cytoskeleton matrix[29].

Another significant impact of both secretome proteins of Kp10 and Gh1 was evident from the presence of swollen periplasmic space likely caused by disintegration of the membrane after secretome protein treatment. The mesosome-like structures present in the cytoplasm of the treated bacterial cells are a simple physicochemical process. They are artifacts that are known to form due to chemical deterioration of the membrane during chemical fixation for electron microscopy[30].

The membrane potential, pH gradient, and efflux of ATP were also measured to support the morphological study. DiSC3(5) is a fluorescent dye that is permeable to cationic membranes. In MRSA and VRE cells energized with glucose, rapid quenching of fluorescence was detected upon addition of the dye, showing the generation of membrane potential. After adding the secretome proteins, an increase in the fluorescence intensity of DiSC3(5) was observed in MRSA, indicating that the membrane potential of the cell was dissipated. The dissipation of membrane potential caused by secretome proteins was stronger than vancomycin. However, a decrease in the fluorescence intensity of DiSC3(5) was observed in VRE, indicating cell membrane hyperpolarization. The generation of a pH gradient was analyzed by determining changes in intracellular pH with the BCECF, AM fluorescent probe. The pH reading increased upon addition of Kp10 and Gh1 secretome proteins, indicating depletion of the membrane.

The efflux of ATP caused by secretome proteins of Kp10 and

Gh1 was concentration-dependent. Bacterial replication and ATP generation are both dependent on membrane potential. Membrane potential dissipation may increase membrane permeability, resulting in the loss of cytoplasmic contents such as ATP. ATP leakage causes intracellular ATP depletion, which can result in bacterial death. Surprisingly, the amount of ATP released by MRSA and VRE during secretome protein exposure increased as the concentration of protein increased throughout the study. Bacterial ATP can be depleted in cell supernatants, possibly through hydrolysis at their cell surfaces. The current findings suggest that MRSA and VRE treated with secretome proteins of Kp10 and Gh1 retain some ability to degrade extracellular ATP.

In accordance with the inhibitory effects and morphological changes, the presence of secretome proteins of Kp10 and Gh1 also significantly disrupted the general metabolic pathway in MRSA and VRE. In this study, 2D-proteomic analysis was run to analyze the protein expression profile. In MRSA treated with secretome proteins of Kp10 and Gh1, one of the affected protein lost was 50S ribosomal protein L6. The suppression of these proteins inhibits translation, thus preventing cell growth, as the ribosomal proteins are crucial and important in protein synthesis in the cells[31].

Another interesting protein that was downregulated in MRSA is alcohol dehydrogenase. This protein was important as *S. aureus* species mostly derive energy from glucose catabolism through glycolysis and Krebs cycles[32]. Alcohol dehydrogenase is found in many bacteria undergoing fermentation[33]. This shows that the loss of these proteins will weaken the condition of the cells.

For the expression of proteins in VRE treated with Kp10 secretome proteins, one of the downregulated proteins is elongation factor Ts. Elongation factor Ts plays an important role in bacterial cells; for instance, its capacity to increase the rate of the ternary complex formation may increase the maximum rate of translation in a cell[34]. Besides, under steady-state conditions, the capacity of elongation factor Ts to facilitate nucleotide turnover may allow for translational control under changing cellular conditions[34].

In the presence of gluconeogenic substrates, class Ⅱ fructose-bisphosphate aldolase is required for bacterial multiplication in macrophages[35]. This protein, however, was downregulated in the VRE cells. Based on their amino acid sequence, class Ⅱ fructose-bisphosphate aldolases are further classified into types A and B aldolases. Type A aldolases are mostly involved in glycolysis and gluconeogenesis, whereas type B aldolases serve a variety of metabolic functions[36].

Exposure of VRE culture to the secretome proteins of Kp10 and Gh1 also suppressed chaperonin family proteins, which include the 60 kDa chaperonin and the chaperone protein DnaK. Chaperonins are important in supporting the folding of newly synthesized proteins, preventing protein aggregation during heat shock, and repairing heat-damaged or misfolded proteins that should not be found in the final protein structure[37]. DnaK interacts with a nascent polypeptide using the cofactor DnaJ, an HSP40 homolog[38]. DnaJ is necessary for DnaK to bind to the polypeptide chain and accelerates the hydrolysis of ATP bound to DnaK[39]. The release of the polypeptide chain is then assisted by GrpE in the presence of ATP[40]. Loss of DnaK may increase the dependence of chaperonin machinery on GroEL/GroES in some bacteria, indicating some communication between different chaperone/chaperonin pathways[41].

As for the limitation, this study only tested against MRSA and VRE strains using the total extract of the secretome proteins of Kp10 and Gh1. Therefore, the efficacy of both secretome proteins against a wider microbial group and the secretome exact components remains unknown and warrants further studies.

With the rapid development of antibiotic resistance in microbes, the ability of AMPs in secretome proteins to induce delayed resistance makes them an extremely promising therapeutic agent. In this respect, secretome proteins are among the most intensively studied as alternatives to antibiotics and promising antimicrobial agents. Based on cell viability studies, MIC, MBC, and time-to-kill assay, we observed that the secretome proteins of Kp10 and Gh1 had antibacterial activity and were shown to reduce the growing number of VRE and MRSA by damaging the cell membrane. Based on microscopic analysis and proton motive study, bacterial cells that were treated with these secretome proteins expressed various phases of cell death ranging from cell membrane disruption to lysis.

These results were in accordance with the patterns of protein expression in MRSA and VRE cells treated with the secretome proteins of Kp10 and Gh1. In this study, we examined the expression of protein and investigated the inhibition mechanism involved by 2D gel proteomic analysis using LCMS to understand the complex effects of both secretome proteins on MRSA and VRE.

Essentially, in the Kp10 and Gh1 secretomes-treated MRSA and VRE, cell division and cell wall biosynthesis/protein synthesis were involved in the inhibition mechanism. The differential expression of proteins observed in this study provided valuable insight into the mechanisms by which growth and pathogenicity in MRSA and VRE were inhibited and confirms the multifactorial effects of the secretome proteins of Kp10 and Gh1 on bacterial cells. Results of this study support the hypothesis that secretome proteins of Kp10 and Gh1 reduce the fitness of MRSA and VRE to inhibit resistant bacterial infections.

Conflict of interest statement

The authors declare no conflict of interest.

Funding

This study was supported by the funds of Ministry of Higher Education, Malaysia and Universiti Putra Malaysia through Fundamental Research Grant Scheme (FRGS/1/2017/SKK11/UPM/01/1) and Putra Grant (GP/2017/9571800).

Authors' contributions

NHZB and MNMD conceived and designed the methodology and data analysis, performed the experiments, prepared figures and/or tables, authored or reviewed drafts of the paper, and approved the final draft. NFKM and NR conceived and designed the experiments, performed the experiments, analyzed the data, authored or reviewed drafts of the paper, and approved the final draft. MMJA, SA, and WAKWNI conceived and designed the experiments, analyzed the data, authored or reviewed drafts of the paper, and approved the final draft. MHY, AMH, and SM analyzed the data, authored or reviewed drafts of the paper, and approved the final draft. AM and NDD conceived and designed the experiments, analyzed the data, prepared figures and/or tables, authored or reviewed drafts of the paper, and approved the final draft.

References

[1] Ventola CL. The antibiotic resistance crisis part 1: Causes and threats. *P T* 2015; **40**(4): 277-283.

[2] Dadgostar P. Antimicrobial resistance: Implications and costs. *Infect Drug Resist* 2019; **12**: 3903-3910.

[3] Zainal Baharin NH, Khairil Mokhtar NF, Mohd Desa MN, Gopalsamy B, Mohd Zaki NN, Yuswan MH, et al. The characteristics and roles of antimicrobial peptides as potential treatment for antibiotic-resistant pathogens: A review. *PeerJ* 2021; **9**: e12193. doi: 10.7717/peerj.12193.

[4] Golkar Z, Bagasra O, Pace DG. Bacteriophage therapy: A potential solution for the antibiotic resistance crisis. *J Infect Dev Ctries* 2014; **8**(2): 129-136.

[5] Sengupta S, Chattopadhyay MK, Grossart HP. The multifaceted roles of antibiotics and antibiotic resistance in nature. *Front Microbiol* 2013; **4**: 47.

[6] Wright GD. Something old, something new: Revisiting natural products in antibiotic drug discovery. *Can J Microb* 2014; **60**(3): 147-154.

[7] Damayanti RH, Rusdiana T, Wathoni N. Mesenchymal stem cell secretome for dermatology application: A review. *Clin Cosmet Investig Dermatol* 2021; **14**: 1401-1412.

[8] Kasiri MM, Beer L, Nemec L, Gruber F, Pietkiewicz S, Haider T, et al. Dying blood mononuclear cell secretome exerts antimicrobial activity. *Eur J Clin Invest* 2016; **46**(10): 853-863.

[9] Yagi H, Chen AF, Hirsch D, Rothenberg, Tan J, Alexander PG, et al. Antimicrobial activity of mesenchymal stem cells against *Staphylococcus aureus*. *Stem Cell Res Ther* 2020; **11**(1): 1-12.

[10] Harman RM, Yang S, He MK, Van de Walle GR. Antimicrobial peptides secreted by equine mesenchymal stromal cells inhibit the growth of bacteria commonly found in skin wounds. *Stem Cell Res Ther* 2017; **8**(1): 1-14.

[11] Kumar P, Kizhakkedathu JN, Straus SK. Antimicrobial peptides: Diversity, mechanism of action and strategies to improve the activity and biocompatibility *in vivo*. *Biomolecules* 2018; **8**(1): 4.

[12] Vieco-Saiz N, Belguesmia Y, Raspoet R, Auclair E, Gancel F, Kempf L, et al. Benefits and inputs from lactic acid bacteria and their bacteriocins as alternatives to antibiotic growth promoters during food-animal production. *Front Microbiol* 2019; **10**: 57.

[13] Mokhtar NFK, Hashim AM, Hanish I, Zulkarnain A, Raja Nhari RMH, Abdul Sani AA, et al. The discovery of new antilisterial proteins from *Paenibacillus polymyxa* Kp10 *via* genome mining and mass spectrometry. *Front Microbiol* 2020; **11**: 1-11.

[14] Jawan R, Abbasiliasi S, Tan JS, Kapri MR, Mustafa S, Halim M, et al. Evaluation of the estimation capability of response surface methodology and artificial neural network for the optimization of bacteriocin-like inhibitory substances production by *Lactococcus lactis* Gh1. *Microorganisms* 2021; **9**(3): 579.

[15] Jawan R, Abbasiliasi S, Tan JS, Mustafa S, Halim M, Ariff AB. Influence of culture conditions and medium compositions on the production of bacteriocin-like inhibitory substances by *Lactococcus lactis* Gh1. *Microorganisms* 2020; **8**(10): 1454.

[16] Arjyal C, Kc J, Neupane S. Prevalence of methicillin-resistant *Staphylococcus aureus* in shrines. *Inter J Microbiol* 2020; **2020**: 7981648. doi: 10.1155/2020/7981648.

[17] Kasimin ME, Mohd Faik AA, Jani J, Abbasiliasi S, Ariff A, Jawan R. Probiotic properties of antimicrobial-producing lactic acid bacteria isolated from dairy products and raw milk of Sabah (Northern Borneo), Malaysia. *Malay App Biol* 2020; **49**(3): 95-106.

[18] Duong-Ly KC, Gabelli SB. Salting out of proteins using ammonium sulfate precipitation. *Methods Enzymol* 2014; **541**: 85-94.

[19] Elshikh M, Ahmed S, Funston S, Dunlop P, McGaw M, Marchant R, et al. Resazurin-based 96-well plate microdilution method for the determination of minimum inhibitory concentration of biosurfactants. *Biotechnol Lett* 2016; **38**(6): 1015-1019.

[20] Wang D, Zhang W, Wang T, Li N, Mu H, Zhang J, et al. Unveiling the mode of action of two antibacterial tanshinone derivatives. *Inter J Mol Sci* 2015; **16**(8): 17668-17681.

[21] Guihard G, Bénédetti H, Besnard M, Letellier L. Phosphate efflux through the channels formed by colicins and phage T5 in *Escherichia coli* cells is responsible for the fall in cytoplasmic ATP. *J Biol Chem* 1993; **268**(24): 17775-17780.

[22] Al-Obaidi JR, Saidi NB, Usuldin SRA, Rahmad N, Zean NGB, Idris AS. Differential proteomic study of oil palm leaves in response to *in vitro* inoculation with pathogenic and non-pathogenic *Ganoderma* Spp. *J Plant Path* 2016; **98**(2): 235-244.

[23] Fisol AFBC, Saidi NB, Al-Obaidi JR, Lamasudin DU, Atan S, Razali N, et al. Differential analysis of mycelial proteins and metabolites

from *Rigidoporus microporus* during *in vitro* interaction with *Hevea brasiliensis*. *Microb Ecol* 2022; **83**(2): 363-379.

[24]Matlow AG, Shaun KM. Control of antibiotic-resistant bacteria in the office and clinic. *Can Med Assoc J* 2009; **180**(10): 1021-1024.

[25]Fair RJ, Tor Y. Antibiotics and bacterial resistance in the 21st century. *Perspect Med Chem* 2014; **28**(6): 25-64.

[26]Mahlapuu M, Håkansson J, Ringstad L, Björn C. Antimicrobial peptides: An emerging category of therapeutic agents. *Front Cell Infect Microbiol* 2016; **6**: 194.

[27]Price-Whelan A, Poon CK, Benson MA, Eidem TT, Roux CM, Boyd JM, et al. Transcriptional profiling of *Staphylococcus aureus* during growth in 2 M NaCl leads to clarification of physiological roles for Kdp and Ktr K^+ uptake systems. *mBio* 2013; **20**; 4(4): e00407- e00413.

[28]da Silva A Jr, Teschke O. Effects of the antimicrobial peptide PGLa on live *Escherichia coli*. *Biochim Biophys Acta* 2003; **1643**(1-3): 95-103.

[29]Li J, Koh JJ, Liu S, Lakshminarayanan R, Verma CS, Beuerman RW. Membrane active antimicrobial peptides: Translating mechanistic insights to design. *Front Neurosci* 2017; **11**: 73.

[30]Balkwill DL, Stevens SE. Effects of penicillin G on mesosome-like structures in *Agmenellum quadruplicatum*. *Antimicrob Agents Chemother* 1980; **17**(3): 506-509.

[31]Dai X, Zhu M, Warren M, Balakrishnan R, Patsalo V, Okano H, et al. Reduction of translating ribosomes enables *Escherichia coli* to maintain elongation rates during slow growth. *Nat Microbiol* 2016; **12**(2): 16231.

[32]Balasubramanian D, Harper L, Shopsin B, Torres VJ. *Staphylococcus aureus* pathogenesis in diverse host environments. *Pathog Dis* 2017; **75**(1): ftx005.

[33]Nosova T, Jousimies-Somer H, Kaihovaara P, Jokelainen K, Heine R, Salaspuro M. Characteristics of alcohol dehydrogenases of certain aerobic bacteria representing human colonic flora. *Alcohol Clin Exp Res* 1997; **21**(3): 489-494.

[34]Burnett BJ, Altman RB, Ferrao R, Alejo JL, Kaur N, Kanji J, et al. Elongation factor Ts directly facilitates the formation and disassembly of the *Escherichia coli* elongation factor Tu·GTP·aminoacyl-tRNA ternary complex. *J Biol Chem* 2013; **288**(19): 13917-13928.

[35]Ziveri J, Tros F, Guerrera IC, Chhuon C, Audry M, Dupuis M, et al. The metabolic enzyme fructose-1,6-bisphosphate aldolase acts as a transcriptional regulator in pathogenic *Francisella Nat Commun* 2017; **8**(1): 853.

[36]Lv GY, Guo XG, Xie LP, Xie CG, Zhang XH, Yang Y, et al. Molecular characterization, gene evolution, and expression analysis of the fructose-1, 6-bisphosphate aldolase (FBA) gene family in wheat (*Triticum aestivum* L.). *Front Plant Sci* 2017; **8**: 1030.

[37]Saibil H. Chaperone machines for protein folding, unfolding and disaggregation. *Nat Rev Mol Cell Biol* 2013; **14**(10): 630-642.

[38]Fourie KR, Wilson HL. Understanding GroEL and DnaK stress response proteins as antigens for bacterial diseases. *Vaccines (Basel)* 2020; **8**(4): 773.

[39]Liberek K, Marszalek J, Ang D, Georgopoulos C, Zylicz M. *Escherichia coli* DnaJ and GrpE heat shock proteins jointly stimulate ATPase activity of DnaK. *Proceed Nat Acad Sci USA* 1991; **88**(7): 2874-2878.

[40]Mayer MP, Bukau B. Hsp70 chaperones: Cellular functions and molecular mechanism. *Cell Mol Life Sci* 2005; **62**(6): 670-684.

[41]Brehmer D, Gässler C, Rist W, Mayer MP, Bukau B. Influence of GrpE on DnaK-substrate interactions. *J Bio Chem* 2004; **279**(27): 27957-27964.

Publisher's note